Vocal fold wave velocity in the cover and body layers measured *in vivo* using dynamic sonography

Chen-Gia Tsai[1*], Tzu-Yu Hsiao[2], and Yio-Wha Shau[3]

[1]Graduate Institute of Musicology, National Taiwan University, Taipei, Taiwan
[2]Departments of Otolaryngology, College of Medicine, National Taiwan University, Taipei, Taiwan
[3]Institute of Applied Mechanics, National Taiwan University, Taipei, Taiwan

ABSTRACT

Traditionally, application of ultrasound imaging on vocal fold vibration has been limited by the frame rate of dynamic sonography. When the frame rate f_s is lower than half of the vibration frequency, ambiguity in the vibration frequency evident from dynamic sonography occurs. This ambiguity is known as *aliasing*. We exploited the aliasing effect in dynamic 2D-mode sonography to capture the vibratory pattern of the vocal fold during modal phonation. The phonation frequency f was tuned to be close to an integer multiple of f_s, so that $f = Nf_s + p$, with N = 2, 3, 4, 5, and 1 Hz < p < 4 Hz. The vibration frequency evident from dynamic sonography was p, and slowly-traveling waves were observed on the vocal fold surface and in the vocal ligament. To measure their propagation velocities, we derived the equation relating the wavelength evident from dynamic sonography, the line-scanning velocity of 2D-mode ultrasound, the phonation frequency, and the wave velocity. The wavelengths evident from dynamic sonography were measured for 90 Hz < f < 203 Hz in a male subject. Our data of the vocal-fold surface wave velocity agreed with previous experiments, whereas measurements of the wave velocity in the vocal ligament agreed with the shear wave velocity estimated from its Young's modulus and density.

INTRODUCTION

Measuring the wave velocity in biological media is a promising method to estimate their mechanical properties. Whereas ultrasound techniques have been widely used to investigate wave propagation in bones (Foldes et al. 1995), arteries (Brands et al. 1998, Eriksson 2002), muscles (Levinson et al. 1995, Gennisson et al. 2003), and tendons (Hoffmeister et al. 1996, Pourcelot et al. 2005), their application on laryngeal examinations has been limited. Lack of interest in ultrasonic imaging of vibrating vocal folds is partly due to the temporal

* Correspondence should be addressed to C.G. Tsai (Graduate Institute of Musicology, National Taiwan University. No.1, Sec. 4, Roosevelt Road, Taipei, Taiwan 106. Tel: +886-2-33664699. Fax: +886-2-23696773. E-mail: tsaichengia@ntu.edu.tw)

resolution and the dynamic response to tiny high-frequency movements. The frame rate of 2D-scan ultrasound (< 50 Hz) is always lower than the phonation frequency (> 80 Hz). When the frame rate f_s is lower than half of the vibration frequency, ambiguity in the vibration frequency evident from dynamic sonography occurs. This ambiguity is known as *aliasing*. A similar effect is seen in films where wagon wheels can appear to be going backwards due to the low frame rate of the film, causing misinterpretation of the movement of the wheel spokes. Nevertheless, it is common to intentionally allow aliasing. An example is the stroboscopic video of the human vocal folds widely used in clinical examinations. The stroboscope flashing rate is tuned to be close to a fraction of the vibration frequency of the vocal folds to show slow tissue movements, and thereby their average vibration patterns are captured. In a similar manner, if the subject is able to tune the singing pitch f to be close to an integer multiple of f_s during ultrasonic imaging, slowly-traveling, low-frequency waves of the vocal fold will appear in sonography.

The aim of the present study was to measure the wave velocities on the vocal fold surface and in the vocal ligament during modal phonation using 2D-mode ultrasound. The orbits of tissue particles on the vocal fold surface are approximately circles or ellipses, whereas the orbits of the tissue particles in the vocal ligament are approximately vertical lines (Tsai et al. 2006). In dynamic sonography of the vocal fold, phase differences between the inferior portion and superior portion can be noted both on the surface and in the vocal ligament (Fig. 1). Most measurements of the propagation velocity of the vocal fold surface waves (or the *mucosal waves*) were performed in the canine larynx (Sloan et al. 1993, Titze et al. 1993, Nasri et al. 1994, see but Shau et al. 2001), whereas no measurements of the wave velocity in the vocal ligament have been reported. In the present study, we proposed an "aliasing ultrasonic imaging method" to measure the wave velocities in the cover and body layers.

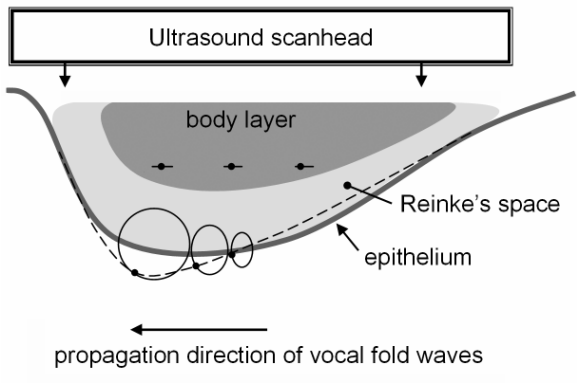

FIG. 1: Coronal view of the right vocal fold showing the tissue motion in the cover and body layers. Vocal-fold waves propagate superiorly in both layers, and there are phase differences between the inferior portion and superior portion. The static shape of the epithelium is represented by the bold curve, while an example of its vibrating shape is represented by the dashed curve.

MATERIALS AND METHODS

Measurements of the line-scanning velocity of 2D-mode ultrasound

A vibrating bar system was used to measure the line-scanning velocity of 2D-mode ultrasound. This system consisted of a metal bar of 3 cm length and a vibratory motor capable of delivering vibration frequencies ranging from 10 to 50 Hz under voltage supply of 1.2 to 4 V with a fixed displacement amplitude of 7 mm. This bar was firmly attached to the motor and immersed in a water container at 6 cm above the bottom surface to reduce the interference of US reflection. A regular medical high-resolution US scanner (HDI-5000, ATL, Bothell, WA) with a linear-array transducer (CL10-5 25 mm, ATL) was used to record the 2D-mode images. This US transducer was placed at about 15 mm above the bar. To see the effect of 2D-mode frame rate on the line-scanning velocity, the vibrating bar was visualized at four frame rates: f_s = 32, 36, 40, and 44 Hz. The vibration frequency of the bar was tuned to be very close to f_s, so that the dynamic sonography was almost stationary. Because of a finite line-scanning velocity U, the visualized vibrating bar was quasi-sinusoidally shaped, and U equals the visualized wavelength L times the vibration frequencies f_s.

Ultrasonic imaging of vocal fold vibration

One of the authors (CG Tsai), a healthy man aged 35 without voice disorders was the subject of this study. The ultrasound scanhead was placed by the subject's left hand in coronal plane at the midline of the thyroid cartilage lamina on the right side (Fig. 1). 2D-mode images were recorded at the frame rates f_s = 32, 36, 40, and 44 Hz during steady modal phonation. In each session of sonographic recording, the phonation frequency f was carefully tuned so that

$$f = Nf_s + p\,. \tag{1}$$

with N = 2, 3, 4, 5, and 1 Hz < p < 5 Hz. For modal phonation, f ranged from 90 Hz to 203 Hz, and there were ten sessions of sonographic recording. As a result of aliasing, the vibration frequency evident from dynamic sonography was p, and the visualized waves propagated slowly from inferior portions of the vocal fold to the superior portions. Because experimental errors resulted mainly from the unsteadiness in f, it is important to maintain the stability of f. This was achieved by real-time visual feedback from sonography. The subject controlled his voice so that the visualized vocal fold waves traveled at a nearly constant velocity.

The visualized wavelengths of the vocal fold waves were extracted from dynamic sonography. In some cases, a single 2D-mode frame showed a complete wavelength on the air-mucosa interface. This method, however, could not be applied to the body waves of the vocal fold, because the tissue particles displace in the same direction as the wave propagation and it is difficult to determine their phase relation from a single frame. In general, we constructed vertical and horizontal M-mode profiles from 2D-mode images to

estimate the visualized wavelengths. Fig. 2 schematically illustrates a horizontal M-mode profile, which presents the phase relation of horizontally-vibrating speckles on a line in the vocal fold body. The visualized wavelengths λ' can be estimated from the visualized vibration period and the equal-phase line.

It should be noted that the horizontal M-mode profiles constructed from 2D-mode images differ from vertical M-mode profiles in their non-simultaneous visualization. To determine the visualized wavelengths of cover waves, a series of vertical M-mode profiles at the air-mucosa interface were constructed from 2D-mode images, which showed the phase relation of epithelium particles.

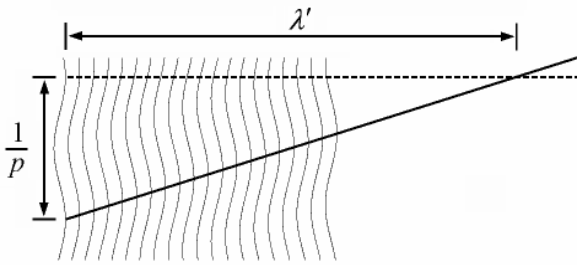

FIG. 2: Measurements of the visualized wavelength λ' and visualized period 1/p from a horizontal M-mode profile, which is constructed from 2D-mode sonography. The solid line represents the equal-phase line.

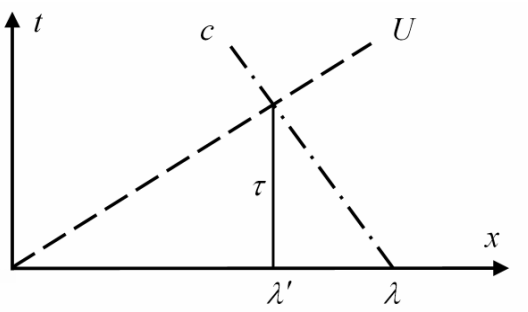

FIG. 3: Schematic description of the effect of wavelength-contraction in 2D-mode sonography. Slopes of the dash and dash-dot lines represent c and U, respectively.

For precise measurements of the phonation frequency *f*, we extracted the vibration frequency evident from dynamic sonography *p* from M-mode profiles. The frame number per visualized period, denoted by *K*, is related to the visualized vibration period 1/*p* by

$$\frac{K}{f_s} = \frac{1}{p}. \tag{2}$$

To construct M-mode profiles from 2D-mode images, a series of horizontal M-mode profiles were constructed on 4 equally-distant lines in the body layer with the inter-distance of 0.2 mm (4 or 5 pixels), and another series of vertical M-mode profiles on 15-17 equally-distant lines that intersected with the air-mucosa interface were constructed with the inter-distance of 10 pixels. For the highest frame rate f_s = 44 Hz, the scan depth was smaller than 1.5 cm and the vibration of the air-mucosa interface was not well visualized. Hence, measurements of λ' of mucosal waves were not performed for f_s = 44 Hz.

Data processing

The wave velocity *c* was calculated in terms of *f* and λ'. Because of a finite line-scanning velocity, sonographic visualization of a traveling wave shows a contracted or lengthened wavelength, depending on the relationship between the directions of the line-scanning and wave propagation. Fig. 3 schematically illustrates the effect of wavelength-contraction when the direction of line-scanning is opposite to wave propagation. The actual wavelength λ is related to the visualized wavelength λ' by

$$\lambda = \lambda' + c\tau = \lambda' + c\frac{\lambda'}{U}, \tag{3}$$

or

$$\frac{\lambda}{\lambda'} = 1 + \frac{c}{U}. \tag{4}$$

Substituting $\lambda = c/f$ into Eq. (4) yields

$$c = \frac{U\lambda' f}{U - \lambda' f}. \tag{5}$$

RESULTS

Table 1 presents the measured line-scanning velocities of 2D-mode ultrasound using a vibrating bar system. As expected, the line-scanning velocity *U* increased along with the frame rate f_s. Their ratio $U/f_s = 26 \pm 0.3$ mm is the maximal distance that a scan can cover. This distance is slightly larger than the length of the scanhead (25 mm) because the system needs time for imaging processing after each scan.

TABLE 1: Line-scanning velocity of 2D-mode ultrasound

Frame rate f_s (Hz)	32	36	40	44
Line-scanning velocity *U* (m/s)	0.83	0.94	1.05	1.13

Wave velocities of the vocal fold cover/body layers were calculated using Eq. (5) with the measurements of *U*, *f*, and λ'. The results are displayed in Fig. 4. The tendency that wave velocities increase along with the phonation frequency is evident. The velocities of the body waves were found higher than those of surface waves. Fig. 4 shows that the errors of body wave velocity are very large for $f > 180$ Hz. This was due to high wave velocities. Because their visualized wavelength λ' approached *L*, the denominator of Eq. (5) was

very small and therefore the calculated wave velocity was fairly sensitive to λ'.

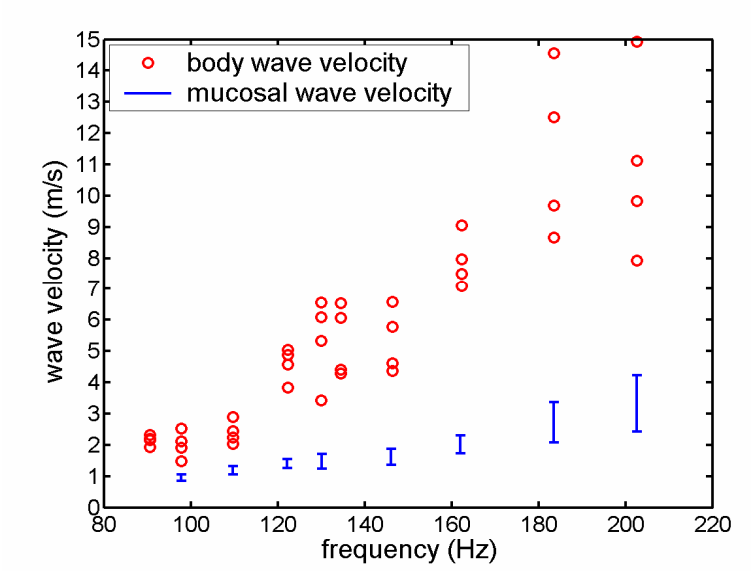

FIG. 4. Measurements of vocal fold wave velocities.

DISCUSSION

Medical ultrasound offers an unusual opportunity to visualize the vibration behavior of the human vocal fold during phonation. In clinical practices, videostroboscopy and high-speed endoscopy have been widely used to visualize the laryngeal activity. Unfortunately, these techniques merely allow for visualization of mucosal waves traveling along the superior surface of vocal folds. Their superior view conceals the medial surface of vocal folds during glottal closure. Moreover, body waves of vocal folds cannot be investigated by endoscopy. While visualizations of the medial surface and the body dynamics of vocal folds have been performed in excised larynx experiments, medical ultrasound may be the unique non-invasive, real-time visualization tool for this task. In our previous studies, the aliasing effect in sonographic visualization was exploited to measure the mucosal wave velocity and the Young's moduli of vocal folds using color Doppler imaging (Shau et al. 2001, Hsiao et al. 2002).

Two major troubles associated with the applications of 2D-mode ultrasound on laryngeal research were successfully solved in the present study. The first one is due to its low frame rates. If the phonation frequency is tuned to be close to an integer multiple of f_s, slowly-traveling, low-frequency waves of the vocal fold will appear in dynamic sonography. Similar to the stroboscopic implementation, performing dynamic sonography over a cycle allows for the estimation of the average vibratory pattern over several successive cycles of actual vocal fold vibration. The visualized wavelength in the sonography can be estimated from M-mode profiles constructed from 2D-mode images. It should be noted that this "aliasing ultrasonic imaging method" is only applicable for periodic tissue vibration, and the majority of errors stem from the unsteadiness in the vibration frequency. The second trouble is due to a finite line-scanning velocity of ultrasound. A frame of 2D-scan does not capture speckles simultaneously. If the direction of line-scanning is opposite to the direction of tissue wave propagation, the visualized wavelength will be shorter than the actual wavelength. We derived the equation relating the visualized wavelength, the line-scanning velocity, the vibration frequency, and the wave velocity [Eq. (5)], and thereby conquered the trouble of non-simultaneous visualization.

Our data of the vocal-fold surface wave velocity agreed with previous experiments performed in canine models (i.e., 0.9 to 1.6 m/s, Sloan et al. 1993; 0.5 to 2.0 m/s, Titze et al. 1993; 0.76 to 2.2 m/s, Nasri et al. 1994), whereas measurements of the wave velocity in the vocal ligament were novel and could be compared to theoretical values. For soft tissues such as the vocal ligament, its bulk modulus is much larger than its shear modulus. Therefore, its vibration is predominated by shear waves at low frequencies if the effects of its pore liquids are neglected. It is appropriate to use the equation of shear wave velocity c_s in elastic media (Love 1944, Achenbach 1973): $c_s = \sqrt{G/\rho_b}$, where G is the shear modulus and ρ_b is the density of the vocal fold body. Here we ignore the viscosity effects, anisotropy and inhomogeneity in this layer. In a soft tissue, Poison ratio is very close to 0.5 and Young's modulus E can be approximated as $3G$. To estimate the shear wave velocity for low-pitched phonation, we choose E = 33 kPa (Min et al. 1995) and ρ_b = 1000 kg/m^3, obtaining $c_s = \sqrt{E/3\rho_b}$ ~ 3.2 m/s. This value agrees with the measured data for 90 Hz < f < 120 Hz (Fig. 4), supporting that the vocal fold body waves are shear waves. For f > 120 Hz, E increases exponentially due to elongation of the vocal ligament (Min et al. 1995), and therefore the shear wave velocity in the vocal fold body also increases exponentially.

Fig. 4 shows that the body wave velocity of the vocal fold is always higher than the mucosal wave velocity. This finding suggests that the phase differences between the cover and body waves are not uniform across the inferior and superior portions of the vocal fold. In a water wave model of vocal fold vibration (Tsai et al. 2006), the body layer is assumed to be forced by the water waves in Reinke's space to also vibrate. The mucosal wave is initiated along the inferior surface of the vocal fold, and the body wave is initiated in the inferior portion of the vocal fold body with a phase lag to the mucosal wave. This phase lag may be reduced in the superior portion of the vocal fold, because the body wave propagates at a higher velocity than the mucosal wave. This hypothesis and its mechanical implications await future research.

CONCLUSIONS

We developed an ultrasound-based methodology to measure the wave velocities in the cover and body layers of the vocal fold. Our data of the vocal-fold surface wave velocity agreed with previous experiments performed in canine models, whereas measurements of the wave velocity in the vocal ligament agreed with the shear wave velocity estimated from its Young's modulus and density. A future model of vocal fold vibration should account for the dynamics and the interaction of these two waves, which propagate in the same direction and with different velocities.

REFERENCES

Achenbach JD. (1973) Wave Propagation in Elastic Solids (Amsterdam: North Holland New York: Elsevier).

Brands PJ, Willigers JM, Ledoux LAF. (1998) A noninvasive method to estimate pulse wave velocity in arteries locally by means of ultrasound. Ultrasound Med Biol 24(9):1325–1335.

Eriksson A. (2002) Arterial pulse wave velocity with tissue Doppler imaging. Ultrasound Med Biol 28:571–580.

Foldes AJ, Rimon A, Keinan DD, and Popovtzer MM. (1995) Quantitative ultrasound of the tibia: a novel approach for assessment of bone status. Bone (N.Y.) 17(4):363–367.

Gennisson JL, Catheline S, Chaffai S, Fink M. (2003) Transient elastography in anisotropic medium: application to the measurement of slow and fast shear wave speeds in muscles. J Acoust Soc Am. 114(1):536–541.

Hanson DG, Jiang J, D'Agostino M, Herzon G. (1995) Clinical measurement of mucosal wave velocity using simultaneous photoglottography and laryngostroboscopy. Ann Otol Rhinol Laryngol 104:340–349.

Hoffmeister BK, Handley SM, Wickline SA, and Miller JG. (1996) Ultrasonic determination of the anisotropy of Young's modulus of fixed tendon and fixed myocardium. J Acoust Soc Am 100:3933–3940.

Hsiao TY, Wang CL, Chen CN, Hsieh FJ, Shau YW. (2002) Elasticity of human vocal folds measured in vivo using color Doppler imaging. Ultrasound Med Biol 28:1145–1152.

Levinson SF, Shinagawa M, and Sato T. (1995) Sonoelastic determination of human skeletal muscle elasticity. J Biomech 28:1145–1154.

Love AEH. (1944) A Treatise on the Mathematical Theory of Elasticity (New York: Dover).

Min YB, Titze IR, Alipour-Haghighi F. (1995) Stress-strain response of the human vocal ligament. Ann Otol Rhinol Laryngol. 104(7):563–569.

Nasri S, Sercarz JA, Berke GS. (1994) Noninvasive measurement of traveling wave velocity in the canine larynx. Ann Otol Rhinol Laryngol 103:758–766.

Pourcelot P, Defontaine M, Ravary B, Lematre M, Crevier-Denoix N. (2005) A non-invasive method of tendon force measurement. J Biomech 38(10):2124–2129.

Shau YW, Wang CL, Hsieh FJ, Hsiao TY. (2001) Noninvasive assessment of vocal fold mucosal wave velocity using color Doppler imaging. Ultrasound Med Biol 27:1451–1460.

Sloan SH, Berke GS, Garratt BR, Kreiman J, Ye M. (1993) Determination of vocal fold mucosal wave velocity in an in vivo canine model. Laryngoscope 103:947–953.

Titze IR, Jiang JJ, Hsiao TY. (1993) Measurement of mucosal wave propagation and vertical phase difference in vocal fold vibration. Ann Otol Rhinol Laryngol 102:58–63.

Tsai CG, Hsiao TY, Shau YW, Chen JH (2006) Towards an intermediate water wave model of vocal fold vibration: Evidence from vocal-fold dynamic sonography. International Conference on Voice Physiology and Biomechanics, July 12–14 2006, Tokyo, Japan.